Maximizing Coverage for mmWave WLANs with Dedicated Reflectors

Ang Deng, Yuchen Liu, and *Douglas M. Blough*
School of Electrical and Computer Engineering
Georgia Institute of Technology
Atlanta, GA 30332-0765

***Abstract*—To accommodate increasingly intensive application bandwidth demands, mmWave WLAN at 60 GHz has been identified as a promising technology with the potential to achieve Gbps throughput. However, mmWave performance is highly dependent on the signal's line-of-sight (LoS) condition due to its high penetration loss when obstructed. We study the use of dedicated flat passive reflectors to improve coverage in indoor mmWave WLANs through a reflector placement scheme that accommodates any general indoor scenario with pre-deployed ceiling-mounted access points (APs). The reflector locations are efficiently selected among all available vertical surfaces within the indoor environment. Through simulations, we show that deployment of intelligently placed reflectors can improve LoS coverage by up to 10%, which is more than deploying one additional AP. Results are provided to illustrate how different factors affect coverage and insights about preferred reflector placements are provided.**

***Index Terms*—mmWave, WLAN, reflector, placement, coverage, line-of-sight**

I. Introduction

In the past decade, the number of connected devices and traffic demand in wireless networks have grown tremendously. Emerging applications, such as UHD video and VR/AR, will provide even greater demands in the near future. According to a Cisco report, Wi-Fi connection speed is forecasted to triple by 2023 [1]. With growing demand in sight, the use of the 60 GHz millimeter-wave (mmWave) band for wireless local-area network (WLAN) communication has been standardized by IEEE 802.11ad/ay [2].

Although mmWave bands provide enormous capacity for next generation wireless networks, coverage is an issue due to severe penetration loss and blockage effects of mmWave signals [3]–[5]. As a result, existence of line-of-sight (LoS) paths is an important factor in determining mmWave performance and, therefore, most prior work on mmWave WLANs has focused on maximizing LoS conditions. Despite the multipath sparsity in mmWave networks, with strong reflectors made of certain materials, some reflection paths may also achieve good link qualities, thereby enhancing overall network performance. Thus, making use of strong first-order reflection paths could be an effective complementary strategy to further improve coverage, robustness, and performance.

In this work, we study the benefits that can be provided by augmenting the physical environment with dedicated flat metal reflectors. Flat metal reflectors are chosen as the subject of study since they are cheap, easy to obtain, and offer perfect specular reflection [6]. While some prior work has demonstrated experimentally that near-LoS performance can be achieved with flat metal reflectors [19], experimental studies are limited in the number of environments and parameter variations they can evaluate. Herein, we provide a simulation study that estimates the coverage benefits that reflectors can provide with different sizes and numbers of reflectors, with different obstacle densities, and when used in conjunction with a varying number of intelligently-placed access points (APs).

Unlike other works which utilize flat metal reflectors in a deliberately constructed way requiring specific setups for both the AP and the reflectors [6], [7], our work accommodates preexisting AP deployments and makes use of existing surfaces for placing the reflectors. In our performance study, we demonstrate that intelligently placed reflectors bring substantial improvements to mmWave indoor coverage and can replace at least one additional AP with lower-cost reflectors. Reflectors are also easier to redeploy after obstacles, e.g. furniture items, are rearranged in a room, as compared to ceiling-mounted APs [8]–[10]. For these reasons, our study demonstrates that a configuration with a small number of fixed APs and a larger number of movable reflectors is an ideal solution for maximizing coverage in mmWave LAN environments with a moderate to high obstacle density.

The paper is organized as follows. Section II discusses related work. The network and reflection models for the system are presented in Section III. In Section IV, the proposed reflector placement methodology is introduced. Simulations are presented in Section V to evaluate the effectiveness of the methodology. The paper is then concluded in Section VI.

II. Related Work

Existing works that examine the possibility of utilizing reflectors to mitigate the NLoS problem can be categorized into three types: 1) utilizing existing reflective surfaces, 2) using passive reflectors, and 3) using intelligent surfaces. In [11] and [12], the effect that existing reflective surfaces have on the coverage and robustness of indoor 60 GHz connectivity when the LoS path experiences obstruction is analyzed. However, most existing objects in indoor scenarios are not made of highly-reflective materials, which makes it hard to rely on them to produce desired link performance [13], [14].

Schemes that use deliberately placed metal reflectors are presented in [6], [7], and [15]. In [7], outdoor coverage

is enhanced by placing parabolic passive reflectors on top of buildings to reflect incoming signal power to users in the shadowed region. To utilize 60 GHz wireless links to solve the bandwidth problem of data center networking, flat metal plates mounted on the ceiling combined with top-of-rack radios are used to circumvent the NLoS problem in [6]. In [15], a parabolic reflector is placed behind a patch antenna of a handheld device to help counter finger shadowing while operating the device. Compared with the use of existing reflective surfaces, exploiting dedicated passive reflectors is a more dependable way to form high quality links at mmWave frequencies. However, this approach requires planned deployments and, to our knowledge, this problem has not been studied in general indoor settings.

The use of intelligent surfaces to provide coverage by reflecting mmWave signals toward mobile users has also been explored. In [16], AI-powered mmWave reflectors are considered in indoor settings and [17] leverages unmanned aerial vehicle (UAV)-carried intelligent reflectors (IR). Both of these works involve machine learning calculations for directing the wave and thus are more expensive than ordinary passive reflectors. In addition, these reconfigurable intelligent surfaces are still under development, and their design complexity and implementation cost are still open questions.

III. System Overview

We now present the network model, reflector model, and reflection path determination method used in the paper.

A. Ceiling-mounted Multi-AP Deployment

We consider indoor environments and assume that APs are mounted on the ceiling, because this achieves better LoS performance with larger coverage as compared to placing APs at a lower height. Then, we adopt the optimal multi-AP placements from [8], where a shadowing-elimination search algorithm is used to generate the APs' locations in the presence of obstacles, such that the LoS coverage can be maximized with a given number of APs. Assuming that, even with optimal placement, a limited number of APs cannot provide full LoS coverage,[1] we study how deployment of passive dedicated reflectors on existing surfaces can enhance high-rate coverage in indoor settings. Due to the use of narrow-beam directional antennas, the interference effects among different transmission links are ignored. Prior work has shown that the impact of side lobe interference is quite small [18].

B. Reflector Model

In this work, we only consider first order reflections for two reasons. Not only do second or higher order reflections lead to a higher path length and therefore weaker signal, but also the lack of appropriate surfaces for second or higher order reflections impedes it from forming effective indirect paths to the receiver. The search space for reflector placement is delineated by all vertical surfaces in the room. More specifically, that includes the four room walls and the side surfaces of all the obstacles in the room.

It is shown in [19] with physical measurements that the reflected signal from a flat metal plate is approximately the same as the Friis free space loss through the same total distance. Additionally, according to [6], even cheap, lightweight steel plates offer perfect specular reflection, neither degrading energy nor changing path loss characteristics. Therefore, we choose our reflectors to be square shaped flat metal reflectors, and in our modeling we consider the reflection to be lossless.

Figure 1 shows two examples of the reflection path determination process, where Figure 1a shows the case where the reflector is located on a wall and Figure 1b shows the case where the reflector is located on an obstacle. For both cases, the right side is the real room's layout depicted with the solid lines, and the left side is the virtual obstacle's layout after the mirror imaging in dashed lines, divided by the middle dashed line which represents the mirror surface. In Figure 1b, the side of an obstacle is marked by the thick blue line segment on the mirror surface. A reflected path between the AP and the targeted cube is represented by the purple solid line, passing through the reflector location marked by a red X.

The reflected path is calculated by creating a mirror image of the room for every plane defined by the candidate vertical surface, where one side is the original room and the mirror side is all applicable obstacles, APs, and walls replicated in perfect symmetry. The reflected path can then be calculated by connecting the reflected (virtual) AP with the non-reflected target. If the intersection between this line and the vertical surface from which the mirror image is created, is a valid location on the surface and the path is not obstructed by any obstacles (real or reflected), then a valid reflection path exists.

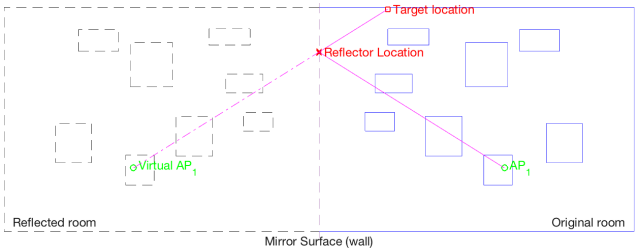

(a) Reflector on the wall.

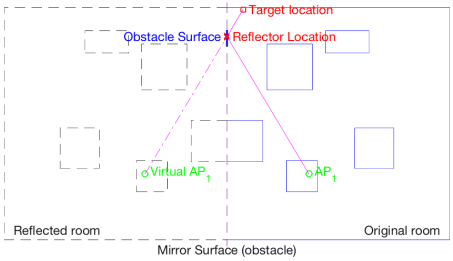

(b) Reflector on an obstacle.

Fig. 1. Examples of the reflection path determination process.

C. Reflector Size

According to the experimental results in [19], the effective area for the reflector size is $A_{refl} = \Delta\Psi\Delta\Omega R_m^2$, where

[1] This is particularly true at relatively high obstacle densities.

$\Delta\Psi$ denotes the angular width in the azimuth plane, $\Delta\Omega$ denotes the angular width in the elevation plane, and R_m is the minimum distance of the receiver antenna from the reflector. In their experiment, the receiver antenna has half-power beam-widths of 26 and 24 degrees in the E and H planes. After fitting the given data points from the paper in a linear fashion, and given our finding that the average distance between a recovered NLoS location from the reflector only ranged from 2.74 m to 3.44 m depending on the obstacle density (the solid line between "Reflector location" and "Target location" in Figure 1), we picked a reflector size of 0.1 m^2 for most of our experiments. This reflector area is supposed to be able to support near Friis free space loss for up to 5.24 m in distance between the receiver antenna and the reflector.

IV. Reflector Placement Methodology

In this section, we introduce a reflector placement algorithm that aims to maximize the network coverage with the given locations of existing APs and obstacle distribution in the scenario. We divide the 3D room into a number of small non-overlapping cubes with side length c_l[2]. Our goal is to maximize the number of cubes that have either LoS or a strong single-reflected path to at least one AP in the network scenario.

Algorithm 1 Check LoS status for a cube

Input: OBs (obstacles' positions), APs (AP's positions), $cube$ (cube location), params (includes r_w, r_l, r_h, size of each obstacle)

Output: AP_{LoS}

1: **for each** $ap\ i \in APs$ **do**
2: $LoS_{ap} = 1$ // init
3: **repeat**
4: **if** $ob \in OBs$ blocks the LoS path between $cube$ and $ap\ i$ **then**
5: $LoS_{ap} = 0$
6: **end if**
7: **until** $LoS_{ap} = 0$ or finished iterating through OBs
8: **if** $LoS_{ap} = 1$ **then**
9: AP_{LoS}.add($ap\ i$)
10: **end if**
11: **end for**
12: **return** AP_{LoS}

Algorithm 1 is an approach that returns all available APs' positions that have LoS connectivity to a target cube with the specific obstacle layout and AP configuration in a room. For each deployed AP, the algorithm loops over every obstacle until an obstacle is found to block the LoS path between the AP and the target cube (Line 3-7). While performing a search for each AP, if none of the obstacles creates obstruction between the AP and the target cube, it implies that there exists LoS connectivity between this AP and the target cube, and all the APs that satisfy this requirement will be added in AP_{LoS} (Line 8-10). Otherwise, when none of the APs can provide LoS connectivity to this cube, AP_{LoS} will be returned as empty.

[2]A smaller c_l provides more accurate results but has higher computational cost.

Algorithm 2 Reflector placement algorithm

Input: N_{ref}, $size_{ref}$, OBs (obstacles' positions), APs (AP's positions), C (cube set), l_g(grid length), params (includes r_w, r_l, r_h, size of each obstacle)

Output: P_{ref}

1: **for each** $cube\ i \in C$ **do**
2: $hasLoS$ = CheckLoS(OBs,APs,$cube$,params)
3: **if** $hasLoS$ is False **then**
4: $NLoS_{Set}$.add(cube i)
5: **end if**
6: **end for**
7: **for** $surf\ i \in$ all vertical surfaces in the room **do**
8: Construct the mirrored room containing reflected obstacles and AP location(s) with regard to $surf\ i$
9: **for each** $cube\ j \in NLoS_{Set}$ **do**
10: AP_{LoS} = Algorithm1(OBs,APs,$cube\ j$,params)
11: **for each** $ap\ k \in AP_{LoS}$ **do**
12: $point$ = the intersect of the straight line defined by $ap\ k$ and $cube\ j$ with $surf\ i$
13: **if** $point$ inside $surf\ i$ boundaries **then**
14: $cubes_{dict}(surf\ i, point) \leftarrow cube\ j$
15: **end if**
16: **end for**
17: **end for**
18: **end for**
19: **for** for each reflector i from 1 to N_{ref} **do**
20: **for** $surf\ j \in$ all vertical surfaces in the room **do**
21: **for** $P_{ref} \in$ all candidate locations in $surf\ j$ **do**
22: $cubes_{set_i} =$ all $(surf\ j, point)$ pairs where $cubes_{dict}(surf\ j, point) \in NLoS_{Set}$
23: **end for**
24: **end for**
25: $ref_i = \arg\max \{cubes_{set_i}\}$
26: $NLoS_{Set}$.delete($cubes_{set_i}$)
27: P_{ref}.add(ref_i)
28: **end for**
29: **return** P_{ref}

Algorithm 2, described in detail below, is an efficient heuristic algorithm to find reflector placements with good network coverage given the AP and obstacle locations. A brute-force optimal solution for a given number of reflectors would try all possible combinations of reflector positions. However, there are an exponential number of possible combinations, meaning an exhaustive search is infeasible for more than a few reflectors. Algorithm 2 places reflectors sequentially by covering as many cubes as possible with each additional reflector.

From a high-level perspective, the proposed searching algorithm is divided into three steps. First, in the actual room, all cubes that do not have LoS under the current AP placement are gathered into $NLoS_{Set}$ (Line 1-6). Therefore, all cubes already having direct LoS connectivity to any APs are excluded from the reflected path search process. Second, based on the list of NLoS cubes, the algorithm builds a mapping between NLoS cubes and surface locations that are capable

of providing a reflected LoS path (if any). Within this section of Algorithm 2 from lines 7 to 18, the rooms are considered as *virtual* rooms constructed through the mirroring process as shown in Figure 1 with respect to each of the vertical surfaces (walls and obstacle sides) (Line 8). The detailed graphical explanation of this reflection process can be found in Section III-B.

More specifically, in the constructed mirrored room, we first check if a cube in $NLoS_{Set}$ has LoS connectivity to any virtual AP (Lines 9-10). If the cube has LoS connectivity in the mirrored room, it means that there is a point on the wall (or obstacle) that offers reflected LoS for the corresponding cube in the actual room. To find that reflection point, in the virtual room, the line connecting each AP that provides LoS between the virtual AP and the original cube is found, and then the intersection point between the line and the mirror surface is calculated (Lines 11-12). Next, the point is checked to see it it falls within the bounds of the actual surface and, if so, it is stored in a hash table whose key is the $(surf, point)$ tuple and the value is the target cube index (Lines 13-15). The basic principle behind finding the reflected point is that, for each surface and a target cube/AP pair, if the cube is able to have connectivity through reflection, there only exists one path to achieve it, i.e., only one location on the surface (if covered by reflector) can produce a single-reflected path.

For each reflector to be placed, the third and final step of the placement algorithm traverses all candidate reflector locations and the reflector location that can eliminate the maximal number of remaining NLoS cubes from $NLoS_{Set}$ is picked as the next reflector location (Lines 20-25). Note that $NLoS_{Set}$ is subsequently updated to ensure that the next reflector placement can eliminate as many NLoS cubes as possible.

V. Performance Study

In this section, we evaluate the coverage improvement that reflectors can bring through the proposed placement approach described in Section IV. In 60 GHz mmWave LAN scenarios, we discuss the coverage improvement with regard to the obstacle density, reflector total area, and reflector size, and we also present a performance comparison of different AP and reflector combinations. Lastly, findings regarding what portion of reflectors end up on obstacles versus walls are presented.

A. Simulation settings

Throughout our simulations and analyses, we consider a fixed-size room of size 9 meters by 6 meters with a height of 3 meters. In the experiments, the number of optimally placed access points, number and size of reflectors, and obstacle density are varied in different sets of experiments. To mitigate the effect of outliers in the results, each plotted data point is an averaged result over 60 experiments.

The performance metric we focus on is the network coverage percentage (NCP), which is the percentage of cubes that have an LoS or a strong single-reflected path to at least one AP over all cubes from the floor to 1.4 m above the floor. The edge length of the cubes c_l is chosen to be 0.1 m, hence each cube's volume is 0.001 m^3.

If not specified otherwise, the parameters used in the following experiments are 60 random layouts of 20 obstacles with about 3 m^2 total reflector area featuring 30 individual reflectors of size 0.316 m × 0.316 m (i.e., an area of 0.1 m^2).

B. Obstacle Model

In our experiments, the obstacles are modeled in a similar way as in [8]. All the obstacles are considered to be cuboids standing on floors and are uniformly distributed within the room. The width and length of obstacles are given by the following truncated normal distributions: $W \sim \mathcal{N}(0.56, 0.08, 0.25, 1.25)$, $L \sim \mathcal{N}(1.08, 0.18, 0.5, 1.75)$, and $H \sim \mathcal{N}(0.76, 0.18, 0.5, 2)$. The orientation of the obstacles is randomly aligned with either the room length or the room width. These parameters were chosen based on a real-life lab environment.

C. The Impact of Reflector Total Area

We first consider a scenario where either 1 AP or 2 APs have been optimally placed through the approach from [8]. There are 20 obstacles in the room and each reflector has an area of 0.1 m^2. In Figure 2, we present the coverage improvement brought by incrementally increasing the total used reflector area A_{ref}, where $A_{ref} = N_{ref} \cdot 0.1$ m^2. In both the single AP and 2 AP cases, as the total area of reflectors increase, the coverage improvement increases. However, the coverage improvement is more rapid at the beginning and the improvement rate monotonically declines as more reflectors are added. The single AP case has a larger absolute coverage value increase compared to the 2 AP case because it starts out at a lower coverage value and therefore has more room for improvement. Figure 2 also includes two horizontal dotted lines which mark the theoretical upper limits achievable through placing reflectors in the room, assuming that an unlimited amount of reflectors are available. The results show that the deployment of reflectors has the potential to improve indoor coverage by substantial amounts (more than 5% for the 2 AP case and more than 10% for the 1 AP case) with a sufficient number of reflectors.

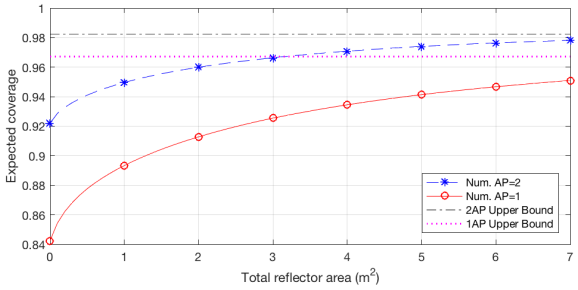

Fig. 2. Line-of-sight coverage vs. total reflector area.

D. The Impact of Obstacle Density

Second, we evaluate the amount of coverage improvement that reflectors can bring to different obstacle densities in the

scenario. In this experiment, we assume that a total of 30 reflectors of size 0.316 m × 0.316 m are deployed in both the 1 AP and 2 AP cases. Figure 3 shows that for both cases, as the number of obstacles increases, the absolute coverage improvement increases as well.

One additional observation that can be made from Figure 3 is that, 3 m^2 of additional reflector area to 1 AP consistently provides roughly equivalent coverage as deploying 2 APs without any reflectors. Therefore, we conclude that in a similar network scenario, choosing 1 AP and some additional reflectors may be a more cost-effective way as compared to deploying 2 APs when the cost of 3 m^2 of reflectors is cheaper than one AP. As noted earlier, reflectors are also considerably easier to redeploy than ceiling-mounted APs providing an additional incentive to use reflectors in place of additional APs.

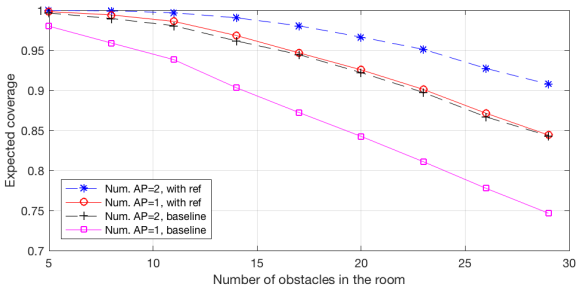

Fig. 3. Line-of-sight coverage vs. obstacle density.

E. The Impact of Reflector Size

We also examine the effect of individual reflector size on the coverage assuming the total area of reflectors is the same. The experiments were set so that the total area of reflectors is 3 m^2, but the individual reflector size ranges from 0.025 m^2 to 0.25 m^2, in step sizes of 0.025 m^2. The value for 0 m^2 shows the upper bound for achievable coverage if the reflectors can be arbitrarily small. Figure 4 shows that the smaller the individual reflector size is, the better is the performance. However, according to the findings in [19], there is a lower limit for the size of reflectors in order to guarantee the signal strength. More specifically, the smallest allowable size is dependent on the distance of the receiver from the reflector. For our average distance between the reflector and the receiver, the minimum allowable size for the reflector is 0.0463 m^2, as marked by the vertical line on Figure 4. Therefore, it would be beneficial when deploying reflectors to find the minimum allowable size to minimize the total area of reflectors used for reaching a target LoS coverage ratio.

F. Evaluating Different Combinations of Reflectors and APs

In the interest of providing a cross comparison between the coverage benefits of additional APs versus additional reflectors for tackling the NLoS problem for indoor mmWave communication, we have collected some corresponding experiment data and formatted it into a table.

We can observe from Table I that, with 15 obstacles in the room, a single AP with the help of 1.7 m^2 of intelligently-

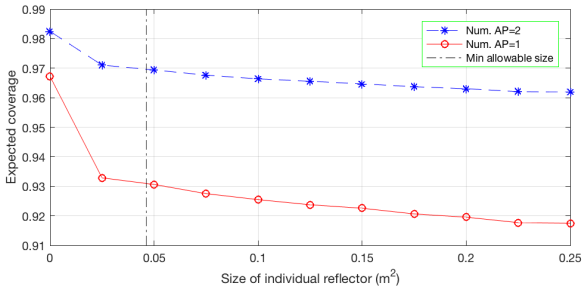

Fig. 4. Line-of-sight coverage vs. size of individual reflector.

placed reflectors can achieve similar performance (95% coverage) as compared to 2 APs. Similarly, with 20 obstacles in the room, 2 APs with 1.1 m^2 of strategically-placed reflectors can achieve coverage equivalent to that of 3 APs. These results show that a certain area of inexpensive metal reflectors can be used in place of an additional AP, with the additional benefit of easier redeployment when the obstacle environment changes. However, it is noted that there are limits to what can be done with reflectors compared to APs. For example, with 25 obstacles, it is not possible to achieve 95% coverage with one AP plus reflectors, whereas 3 APs are able to provide that level of coverage. The dotted lines on Figure 2 demonstrate this point as well, i.e. there is an upper bound to the maximum coverage achievable for a limited number of APs plus an unlimited number of reflectors.

TABLE I
ADDITIONAL REFLECTOR AREA (m^2) TO ACHIEVE 95% COVERAGE

Number of Access Points	Number of Obstacles		
	15	***20***	***25***
1	1.7	6.8	N/A
2	0	1.1	4.9
3	0	0	0.9

G. Reflector Distributions

In this part, we investigate the reflector distributions with our proposed placement approach to maximize network coverage by taking the same results from V-D and analyzing them from a different perspective. Figure 5 shows the top view of an example scenario where there are 8 obstacles and 1 AP (marked by the green circle) in the room. The reflector locations are marked by crosses on the graph, with blue ones on the walls and red ones on the obstacles[3]. It can be seen that much smaller number of reflectors end up on the obstacles than those on the walls.

To further study the reflector distributions and validate this observation, we evaluated various random scenarios with obstacle densities ranging from 5 to 29 and an optimally placed single AP plus 30 reflectors. In Figure 6, we have plotted the ratio of reflectors that are placed on obstacles out of the total number of reflectors. The average percentage of reflectors that end up with a placement on the obstacles' sides

[3]Note that a single location marker may represent a few reflectors of different heights due to overlap.

is 5.08% and those reflectors contribute less than 5% of the the total additional coverage. It can also be observed that as the obstacle density increases, the ratio increases. The ratio increase may be caused by the increase of obstacle surface area to be utilized. We can conclude from this result that even in the case where deploying reflectors on obstacles is impractical, deploying passive reflectors on walls alone can still achieve 95% of the coverage improvement promised in Sections V-C and V-D.

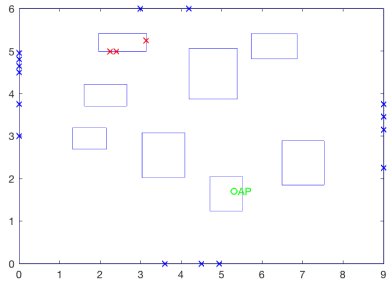

Fig. 5. Example top view of reflector placement scheme.

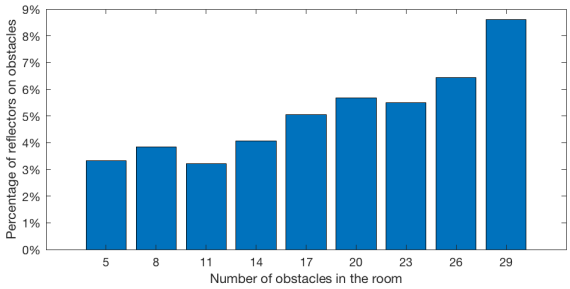

Fig. 6. Percentage of reflectors on obstacles vs. obstacle density.

H. Discussion

Here we summarize the key findings from this section:

- Intelligently deploying 3 m^2 of reflectors with our approach in typical indoor environments can boost network coverage by up to 10%.
- The coverage improvement brought by deploying sufficient reflectors is equivalent to that of deploying 1 or 2 additional APs.
- Given a fixed amount of total reflector area, a smaller size of individual reflectors leads to better coverage performance, but there is a lower bound to the size of the reflector to retain signal power.
- On the cases evaluated, about 95% of reflectors are placed on walls versus on obstacles.

VI. Conclusion

In this work, we explored the use of passive reflectors to improve coverage in indoor mmWave WLANs and proposed a practical yet effective reflector placement scheme. Numerical results show that a reasonable number of intelligently placed reflectors improves coverage by up to 10%. A possible future direction is exploring curve-shaped passive reflectors (e.g. cylinder or sphere-shaped) to further improve mmWave coverage.

Acknowledgement

This research was supported in part by the National Science Foundation through Award CNS–1813242.

References

[1] Cisco, "Cisco Annual Internet Report (2018–2023)," white paper at Cisco.com, Mar. 2014.

[2] IEEE Standard 802.11ad-2012, 2012. URL: https://ieeexplore.ieee.org/servlet/ opac?punumber=6392840.

[3] N. Moraitis and P. Constantinou, "Indoor channel measurements and characterization at 60 GHz for wireless local area network applications," in *IEEE Transactions on Antennas and Propagation*, vol. 52, no. 12, pp. 3180-3189, Dec. 2004.

[4] Y. Liu and D. Blough,"Analysis of blockage effects on roadside relay-assisted mmWave backhaul networks," in *IEEE International Conference on Communications*, 2019.

[5] Y. Liu, and D. Blough, "Blockage robustness in access point association for mmWave wireless LANs with mobility," in *IEEE Conference on Local Computer Networks*, 2020.

[6] X. Zhou, Z. Zhang, Y. Zhu, Y. Li and S. Kumar, et al., "Mirror mirror on the ceiling: Flexible wireless links for data centers," in *ACM SIGCOMM Computer Communication Review*, vol. 42, no. 4, pp. 443–454, 2012.

[7] Z. Peng, L. Li, M. Wang, Z. Zhang and Q. Liu, et al., "An effective coverage scheme With passive-reflectors for urban millimeter-wave communication," in *IEEE Antennas and Wireless Propagation Letters*, vol. 15, pp. 398-401, 2016.

[8] Y. Liu, Y. Jian, R.Sivakumar and D. Blough, "Optimal access point placement for multi-AP mmWave WLANs," in *Proceedings of the 22nd ACM Conference on Modeling, Analysis and Simulation of Wireless and Mobile Systems*, 2019, pp. 35–44.

[9] Y. Jian, M. Agarwal, S. Venkateswaran, Y. Liu, D. Blough, and R. Sivakumar, "WiMove: Toward infrastructure mobility in mmWave WiFi," In *Proceedings of ACM Symposium on Mobility Management and Wireless Access*, 2020.

[10] Y. Liu, Y. Jian, R. Sivakumar, and D. Blough, "On the potential benefits of mobile access points in mmwave wireless LANs," in *IEEE International Symposium on Local and Metropolitan Area Networks*, 2020.

[11] M. Park and H. Pan, "A spatial diversity technique for IEEE 802.11 ad WLAN in 60 GHz band," in *IEEE communications letters*, vol. 16, no. 8, pp. 1260-1262, 2012.

[12] Z. Genc, U. H. Rizvi, E. Onur and I. Niemegeers, "Robust 60 GHz indoor connectivity: Is it possible with reflections?," *IEEE 71st vehicular technology conference*, 2010.

[13] B. Langen, G. Lober, and W. Herzig,"Reflection and transmission behaviour of building materials at 60 GHz," in *Personal, Indoor and Mobile Radio Communications, 1994. Wireless Networks - Catching the Mobile Future., 5th IEEE International Symposium on*, Sep. 1994, vol.2, pp. 505–509.

[14] K. Sato, T. Manabe, T. Ihara, H. Saito and S. Ito, et al., "Measurements of reflection and transmission characteristics of interior structures of office building in the 60-GHz band," in *IEEE Transactions on Antennas and Propagation*, Dec. 1997, vol. 45, no. 12, pp. 1783-1792.

[15] M. Heino, C. Icheln and K. Haneda, "Reflector design to mitigate finger effect on 60 GHz user devices," in *11th European Conference on Antennas and Propagation* , 2017, pp. 151-155.

[16] M. N. Soorki, W. Saad and M. Bennis, "Ultra-reliable millimeter-wave communications using an artificial intelligence-powered reflector," in *IEEE Global Communications Conference*, 2019, pp. 1-6.

[17] Q. Zhang, W. Saad and M. Bennis, "Reflections in the sky: millimeter wave communication with UAV-carried intelligent reflectors," in *IEEE Global Communications Conference*, 2019, pp. 1-6.

[18] Z. Marzi, U. Madhow and H. Zheng, "Interference analysis for mm-Wave picocells," in *IEEE Global Communications Conference*, 2015.

[19] W. Khawaja, O. Ozdemir, Y. Yapici, F.Erden and I. Guvenc, "Coverage enhancement for NLOS mmWave links using passive reflectors," in *IEEE Open Journal of the Communications Society*, Jan. 2020.